Am J Transl Res 2023;15(2):745-754
www.ajtr.org /ISSN:1943-8141/AJTR0144888

Original Article

Bradykinin protects against DDP-induced GP-H1 cell damage via activation of PI3K/Akt/NO signaling pathway

Jingfang Xu[1*], Xinjuan Yin[1*], Yanan Zhang[1], Feng Zhang[1], Xiaobei Tian[1], Qiaona Wu[1], Jie Hu[2], Kexin Wang[3], Zehua Zhang[4], Suwen Su[5], Zengjuan Liu[1]

[1]Department of Pharmacy, The Third Hospital of Shijiazhuang, Shijiazhuang, Hebei, China; [2]Department of Imaging, The Third Hospital of Shijiazhuang, Shijiazhuang, Hebei, China; [3]Department of Pharmacy, The Second Hospital of Hebei Medical University, Shijiazhuang, Hebei, China; [4]Student of Hebei Medical University, Shijiazhuang, Hebei, China; [5]School of Basic Medical Sciences, Hebei Medical University, Shijiazhuang, Hebei, China. [*]Equal contributors and co-first authors.

Received June 21, 2022; Accepted December 27, 2022; Epub February 15, 2023; Published February 28, 2023

Abstract: Objective: To investigate the effect of bradykinin (BK) on cisplatin (DDP)-induced cardiotoxicity at the cellular level and its cytological mechanism. Methods: The toxic effects of DDP on GP-H1 cells, and the effects of BK on DDP cardiomyocyte survival rate, DDP-induced malondialdehyde (MDA), lactate dehydrogenase (LDH), superoxide dismutase (SOD), reactive oxygen species (ROS), mitochondria membrane potential (MMP) and apoptosis were explored. Results: DDP at different concentrations inhibited GP-H1 cells at 12 h after administration, and the inhibitory effect was more prominent at 24 h after administration and continued until 72 h after administration. The severity of GP-H1 cell damage induced by DDP was reduced by 0.1 μM, 1 μM, and 10 μM BK. After GP-H1 cells were treated with DDP, ROS levels increased and MMP levels decreased, while BK intervention inhibited these effects. At 24 h after DDP treatment, Bax/bcl-2 increased in GP-H1 cells, and the expressions of Caspase-3, p-NF-κB, p-p38 and p-Smad2 decreased. After intervention with BK, it was shown that Bax/Bcl-2 was significantly reduced, and the expressions of Caspase-3, p-NF-κB, p-p38 and p-Smad2 decreased. Bax/Bcl-2 and the expressions of Caspase-3, p-NF-κB, p-p38 and p-Smad2 of GP-H1 cells were basically not affected by BK alone. Conclusion: The protective effect of BK on DDP-induced GP-H1 cell damage in guinea pig is related to the activation of PI3K/Akt/NO signaling pathway by BK, which reduces oxidative stress levels in cardiomyocytes and also acts as an anti-apoptotic agent.

Keywords: Bradykinin, cisplatin, cardiotoxicity, effects, molecular cytology, mechanism

Introduction

Cisplatin (DDP) is a chemotherapeutic drug used in the treatment of a variety of solid tumors, including cervical cancer, bladder cancer, testicular cancer, etc., but its clinical application is severely limited due to its serious toxic side effects, such as ototoxicity, nephrotoxicity, cardiotoxicity and neurotoxicity. Although it is commonly used in the treatment of malignant tumors, clinical studies have also found that DDP exhibits an excessive affinity for myocardial tissue while being anti-tumor, leading to an accumulation in cardiomyocytes and inducing cardiotoxicity, thus resulting in its limited clinical application [1, 2]. The main cardiotoxic mechanism of DDP is related to excessive oxidative stress caused by overproduction of myocardial oxygen free radicals. DDP can be reduced to semiquinone DDP in cardiomyocytes, and the latter converts oxygen molecule (O_2) to superoxide anion (O_2^-) with increased production of hydrogen peroxide (H_2O_2) [3]. Increased production of these free radicals can trigger lipid peroxidation, leading to damages to cell membrane structure, DNA and proteins in cardiomyocytes that manifest as inflammatory and apoptotic changes, both of which can limit cardiac function [4]. There is increasing evidence that oxidative stress and inflammation are the main toxic mechanisms of DDP-induced cardiotoxicity, and that inducible nitric oxide synthase

(iNOS)-induced NO and O_2^- are key cellular components of DDP-induced cardiotoxicity [5]. However, the specific molecular cytological mechanism is still unclear.

Bradykinin (BK) is produced by the transformation of kininogen under the action of kinin-releasing enzyme when the body is subjected to pathological stimuli such as tissue damage, hypoxia, and inflammation [6]. The kallikrein-kinin system (KKS) is found in a wide range of animal tissues, and it produces multiple biological effects through various signaling pathways and is involved in the regulation of multiple organ functions and pathophysiological processes, such as cardiovascular, renal and nervous system regulation, as well as cell proliferation, inflammation and apoptosis [7]. KKS attenuates apoptosis and enhances cardiac function [8]. Studies have found that decreased KKS activity is associated with left ventricular hypertrophy, heart failure, hypertension, diabetes and myocardial infarction, confirming that KKS can protect the heart [9, 10]. However, whether there is a correlation between KKS and DDP-related myocardial injury has not been analyzed. It is of great significance to study how to mitigate the cardiotoxicity of DDP in its application.

In this study, we analyzed the role of BK in DDP-induced cardiotoxicity and the possible intracellular signal transduction pathways of BK using a cytotoxicity model of DDP-induced myocardial injury. The clinical significance of this study is to provide a new approach for the treatment of cardiotoxicity, and to give evidence support at a receptor level for the development of highly effective and low-toxicity antitumor drugs.

Materials and methods

Materials

GP-H1 cells were used in this study. The instruments and equipment used in this study included optical microscope (Leica Microsystems GmbH, Wetzlar, Germany), -86°C cryogenic incubator (Thermo Fisher Scientific, Waltham, USA), automatic biochemical analyzer (CHEMIX-180, Shanghai Lishen Scientific Equipment Co., Ltd., China), UV spectrophotometer (Shanghai Anting Scientific Instrument Factory, China), centrifuge (Eppendorf, Hamburg, Germany), constant temperature water bath (Edmund Bühler GmbH, Bodelshausen, Germany), electronic balance (Shanghai Anting Scientific Instrument Factory, China) and pipette (Zealway (Xiamen) Instrument Inc., China). All the antibodies used in this study were bought from Affinity Biosciences, including cleaved-Caspase 3 (No. AF7022, 1:1000), NF-κB (No. AF6217, 1:1000), p-NF-κB (No. AF3219, 1:1000), p38 (No. AF6456, 1:1000), p-p38 (No. AF4001, 1:1000), Smad2 (No. AF6449, 1:500) and p-Smad2 (No. AF3449, 1:1000).

Methodology

Cardiomyocyte culture: The procedures for cardiomyocyte culture included cell culture, medium change and passaging-freeze-thawing of adherent cells.

Determination of DDP toxicity on GP-H1 cells: GP-H1 cells in good conditions and about 85% confluence were selected. The single-cell suspension was prepared by tryptic digestion. Cells were inoculated in a 96-well plate with a density of 5×10^4/mL, 100 μL per well, at saturated humidity, 5% CO_2, 37°C for 1 day of routine incubation, followed by washing with PBS, and adding with 0.1, 0.3, 1, 3, 10 and 30 μm of DDP at 12, 24, 36, 48, 60 and 72 h, respectively, using medium containing fetal bovine serum. Afterwards, 5 mg/mL MTT was added, 20 μL per well and incubated for 5 h. The supernatant was discarded, and each well was added with 150 μL of dimethyl sulfoxide, shaken and mixed well, and wells without cells were set as the blank controls. The multifunctional enzyme immunoassay was used to determine the optical density at 490 nm for three times.

Determination of the viability of GP-H1 cells: The effect of DDP on the viability of GP-H1 cells were determined with similar procedures described above.

Determination of cardiomyocyte survival rate: GP-H1 cells in a good condition at logarithmic growth stage (80-90% confluency) were digested to prepare cell suspension. Cells were inoculated with 5×10^4/mL cells in a 96-well plate, 100 μL per well, and incubated at 37°C, 5% CO_2 and saturated humidity overnight. The cells

were added with 10 μM, 1 μM and 0.1 μM BK for 30 min of incubation, followed by adding with DDP. The cells were grouped into control group, 0.1 μM BK group, 1 μM BK group, 10 μM BK group, 0.1 μM BK+DDP group, 1 μM BK+DDP group, and 10 μM BK+DDP group. The concentration of BK that could inhibit the toxicity of DDP was determined.

Determination of malondialdehyde (MDA), lactate dehydrogenase (LDH) and superoxide dismutase (SOD): GP-H1 cells in a good condition at logarithmic growth stage (80-90% confluency) were divided into four groups: control group, DDP group, DDP+BK group, and BK group. BK was added 30 min before DDP and incubated for 24 h. The supernatant and cell lysate of each group were taken, and the protein concentration was determined with UV spectrophotometer. SOD activity (SOD ELISA kit, No. SP11149) and MDA content (MDA ELISA kit, No. SP10462) in cell lysate and LDH content (LDH ELISA kit, No. SP10961) in supernatant were determined according to the kit instructions. All the kits were purchased from Wuhan Saipei Biotechnology Co., Ltd., China.

Detection of intracellular reactive oxygen species (ROS): A circular coverslip soaked in 75% alcohol was burned on an alcohol lamp and placed in a 24-well plate. GP-H1 cells in a good condition at the logarithmic growth stage (80-90% confluency) were digested to prepare the cell suspension and placed on circular coverslip, 100 μL per well, and then they were incubated at 37°C, 5% CO_2 and saturated humidity for 4 h. After that, 100 μL of culture medium was supplemented in each well and incubated overnight. The cells were grouped into control group, DDP group, DDP+BK group and BK group. BK was added 30 min before DDP and incubated for 24 h. After 24 h of culture in the incubator, the cells were washed twice with PBS. The fluorogenic probe 2,7-dichlorofluorescin diacetate (DCFH-DA) for reactive oxygen molecules (ROS) was diluted to 1 μM and stained for 30 min. The fluorescence density of cells was detected under laser confocal microscopy in FITC mode. DCFH-DA itself is not fluorescent and can freely cross the cell membrane and hydrolyze in the cell to generate DCFH, which in combination with ROS can become fluorescent DCF. Therefore, fluorescence intensity can reflect the ROS level in the cells.

Detection of mitochondrial membrane potential (MMP): GP-H1 cells were treated and grouped as previously described. The fluorogenic probe Rh123 for MMP was diluted to 0.5 μM and stained for 30 min. The fluorescence density of cells was detected under laser confocal microscope in FITC mode. Rh123 is a lipophilic cationic fluorescent dye, which is permeable to cell membrane and can be selectively enriched in mitochondria. When cells are in a viable state, Rh123 is permeable to the cell membrane, accumulates in mitochondria and emits green fluorescence. In the process of apoptosis, the transport capacity and electronegativity of the mitochondrial membrane are decreased, the ability of the cell mitochondria to accumulate Rh123 is also lost, and the fluorescence intensity is reduced. Accordingly, the changes of MMP can be detected to reflect the apoptosis of cells.

Whole cell protein extraction: The whole protein was extracted in the following steps: cell collection and lysis, protein quantification, and protein sample processing. The procedures to determine DDP-induced cell apoptosis were as follows: protein electrophoresis, protein transfer, immunostaining method showing target protein bands, and result analysis.

The mechanism of BK protection against DDP-induced cardiomyocyte injury: (1) The role of PI3K/Akt/NO signaling pathway in BK protection against DDP induced cardiomyocyte injury was analyzed. GP-H1 cells in a good condition at logarithmic growth stage (80-90% confluency) were digested to prepare cell suspension. The cells were inoculated with 5×10^4/mL cells in a 96-well plate, 100 μL per well, and incubated at 37°C, 5% CO_2 and saturated humidity overnight. After BK incubation for 30 min, DDP and B2 receptor inhibitor HOE-140 (H), PI3K inhibitor LY294002 (LY), NOS inhibitor L-NAME (L) and PLC inhibitor U-73122 (U) were added, respectively. The cells were grouped to control group, DDP group, BK+DDP group, BK+DDP+H group, BK+DDP+L group, BK+DDP+LY group and BK+DDP+U group. MTT assay was used to detect the survival rate of each group. (2) The effect of PLC/PI3K/Akt/NO signaling pathway on BK reducing ROS content in cardiomyocytes induced by DDP was analyzed. A circular coverslip soaked in 75% alcohol was burned on an alcohol lamp and placed in a 24-well plate.

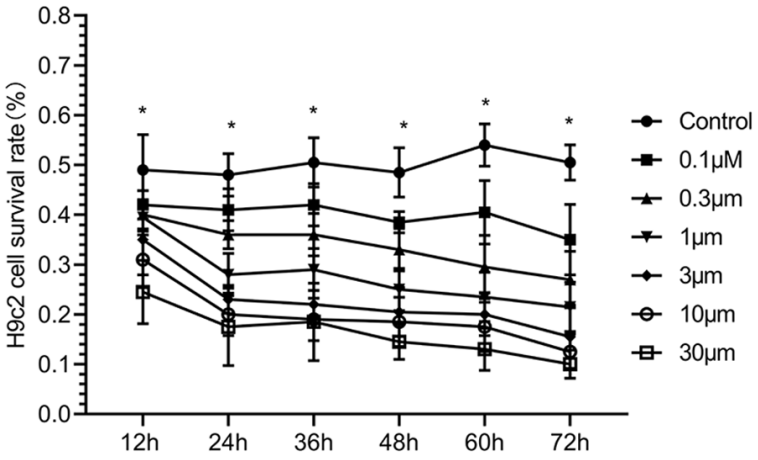

Figure 1. Toxic effects of DDP on GP-H1 cells. The reduction in GP-H1 cell survival in the other six groups was greater than that in the control group at 12 h, 24 h, 36 h, 48 h, 60 h and 72 h, and the survival rate of GP-H1 cells decreased significantly with the increase of concentration ($P < 0.05$). DDP: cisplatin. *$P < 0.05$ compared with control group.

GP-H1 cells in a good condition at the logarithmic growth stage (80-90% confluency) were digested to prepare the cell suspension, placed on circular coverslip 100 μL per well, and incubated at 37°C, 5% CO_2 and saturated humidity for 4 h. After that, 100 μL of culture medium was supplemented in each well and incubated overnight. After incubating with BK for 30 min, DDP and blocking agent were added, and the cells were grouped as previously described. After 24 h of culture in the incubator, the cells were washed twice with PBS. The fluorogenic probe DCFH-DA for ROS was diluted to 1 μM and stained for 30 min. The fluorescence density of cells was detected under a laser confocal microscope in FITC mode. (3) The effect of PLC/PI3K/Akt/NO signaling pathway on BK alleviating MMP in cardiomyocytes induced by DDP was analyzed. GP-H1 cells were treated and grouped as previously described. The fluorogenic probe Rh123 for MMP was diluted to 0.5 μM and stained for 30 min. The fluorescence density of cells was detected under the laser confocal microscope in FITC mode.

Outcomes measures

The toxic effects of DDP on GP-H1 cells and GP-H1 cell viability, the effects of BK on survival rate of cardiomyocyte with the presence of DDP, and the effects of BK on DDP-induced MDA, LDH, SOD, ROS levels, MMP, apoptosis as well as the mechanism of BK protection against DDP-induced cardiomyocyte injury were observed and analyzed.

Statistical analysis

Statistical analyses were performed using Statistical Package for Social Science (SPSS) 23.0 software. Normally distributed measurement data were expressed as mean ± SD, and comparison between two groups was performed by using independent sample *t*-test, comparison between multiple groups by one-way analysis of variance (ANOVA), and pairwise comparison by SNK test. Graphs were plotted using GraphPad Prism 8. $P < 0.05$ was considered statistically significant.

Results

Toxic effects of DDP on GP-H1 cells

GP-H1 cells were incubated with varying concentrations of DDP for 12-72 h, and cell viability was compared by MTT method. It was found that DDP at different concentrations began to inhibit GP-H1 cells at 12 h after administration, and the inhibitory effect was more prominent at 24 h after administration and continued until 72 h after administration. The survival rate of GP-H1 cells decreased significantly with the increase of concentration ($P < 0.05$) (**Figure 1**).

Effect of DDP on the cell viability of GP-H1 cells

The 24 h of incubation with DDP decreased the viability of GP-H1 cells by 50% at a concentration of 1.14 μm, so the DDP injury model was subsequently prepared at a concentration of 1 μm (**Figure 2**).

Effects of BK on viability of DDP-induced cardiomyocytes

The viability of GP-H1 cells was basically unaffected when 0.1 μm, 1 μm and 10 μm BK were applied to GP-H1 cells for 24 h. All the three

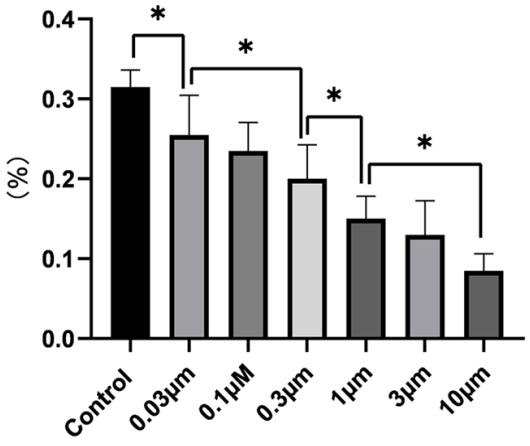

Figure 2. Effect of DDP on the survival rate of GP-H1 cells. The survival rate of GP-H1 cells in the other six groups decreased significantly when compared with that in the control group ($P < 0.05$), and the survival rate of GP-H1 cells showed a downward trend with the increase of drug concentration. DDP: cisplatin. * indicates pairwise comparison, $P < 0.05$.

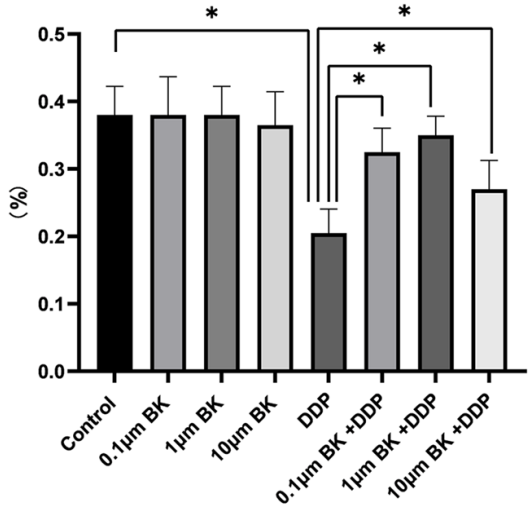

Figure 3. Effect of BK on cardiomyocyte survival rate. The decrease in GP-H1 cell survival rate in the DDP group was lower than that in the control group ($P < 0.05$), and the survival rate was higher in the BK treatment groups than that in the DDP group ($P < 0.05$). The highest survival rate was observed in 1 μm BK group. DDP: cisplatin; BK: bradykinin. * indicates pairwise comparison, $P < 0.05$.

concentrations of BK reduced the DDP-induced damage of GP-H1 cells. To avoid non-specific toxic responses, 0.1 μm BK was used to resist DDP-induced toxicity (**Figure 3**).

Effect of BK on DDP-induced change of MDA, LDH, and SOD levels

After 24 h of treatment with DDP on GP-H1 cells, the levels of LDH in the cell culture medium and the levels of MDA in the cell lysate increased significantly while the SOD activity decreased significantly. Through BK induction, MDA and LDH levels decreased significantly, and SOD activity increased. GP-H1 cells treated with BK alone had no significant effect on MDA and LDH levels and SOD activity (**Figure 4**).

The effect of BK on DDP-induced change of ROS levels

GP-H1 cells were treated with DDP, and the change in ROS level was measured by the ROS-specific fluorescent probe 2,7-DCFH-DA. It was found that DDP could induce an increase in ROS level in GP-H1 cells at 24 h after administration. Continuous half-hour induction with BK prior to the use of DDP resulted in a decrease in cellular ROS levels (**Figure 5**).

Effect of BK on DDP-induced change of MMP levels

GP-H1 cells were treated with DDP, and the changes in MMP at 24 h after DDP administration were measured by Rh123. It was found that DDP significantly reduced the MMP level of GP-H1 cells at 24 h after administration, while half-hour induction with BK before DDP usage increased the MMP level (**Figure 6**).

Effect of BK on DDP-induced apoptosis

After DDP and BK administration to GP-H1 cells, the expressions of apoptotic proteins Bax, Bcl-2 and others were examined by Western blot. It was found that the expression of pro-apoptotic protein Bax was significantly increased, and the expressions of anti-apoptotic protein Bcl-2, Caspase-3, p-NF-κB, p-p38 and p-Smad2 were significantly decreased. There was a significant increase in the level of Bax/Bcl-2 of GP-H1 cells at 24 h after administration. The induction with BK resulted in decreased expression of Bax, increased expression of Bcl-2, and significantly reduced ratio of Bax/Bcl-2. The Bax/Bcl-2 expression of GP-H1 cells was basically not affected by BK alone.

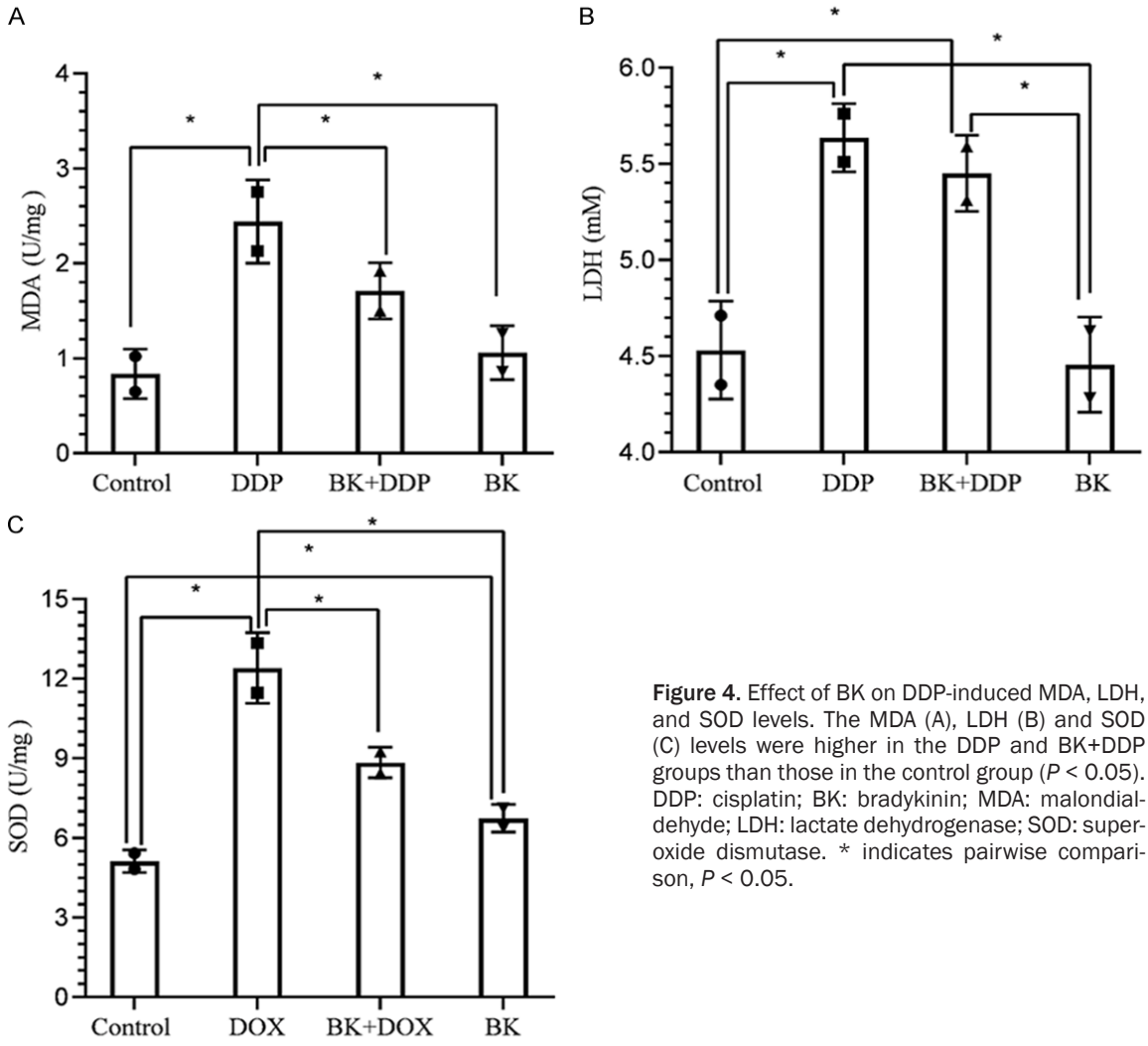

Figure 4. Effect of BK on DDP-induced MDA, LDH, and SOD levels. The MDA (A), LDH (B) and SOD (C) levels were higher in the DDP and BK+DDP groups than those in the control group ($P < 0.05$). DDP: cisplatin; BK: bradykinin; MDA: malondialdehyde; LDH: lactate dehydrogenase; SOD: superoxide dismutase. * indicates pairwise comparison, $P < 0.05$.

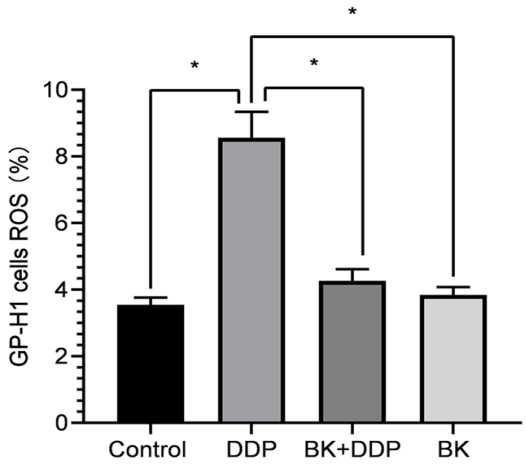

Figure 5. Effect of BK on DDP-induced ROS levels. The ROS levels of GP-H1 cells were higher in the DDP group than that in the control group ($P < 0.05$), while the ROS levels of GP-H1 cells were significantly lower in the BK+DDP group and the BK group than that in the DDP group ($P < 0.05$). DDP: cisplatin; BK: bradykinin; ROS: Reactive Oxygen Species. * indicates pairwise comparison, $P < 0.05$.

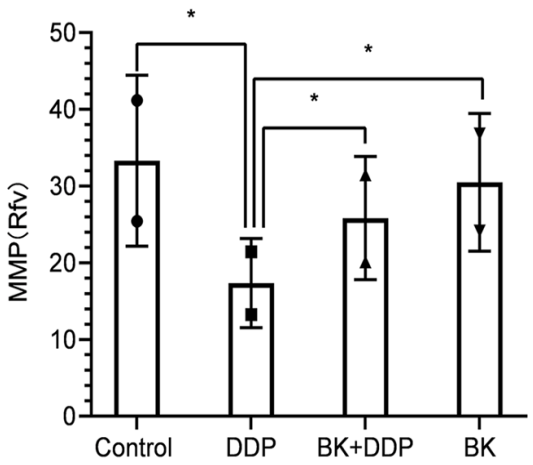

Figure 6. Effect of BK on DDP-induced MMP. Compared with that in the control group, MMP level of GP-H1 cells was lower in the DDP group ($P < 0.05$). Compared with that in the DDP group, MMP levels of GP-H1 cells were higher in the BK+DDP group and the BK group ($P < 0.05$). DDP: cisplatin; BK: bradykinin; MMP: Mitochondria Membrane Potential. * indicates pairwise comparison, $P < 0.05$.

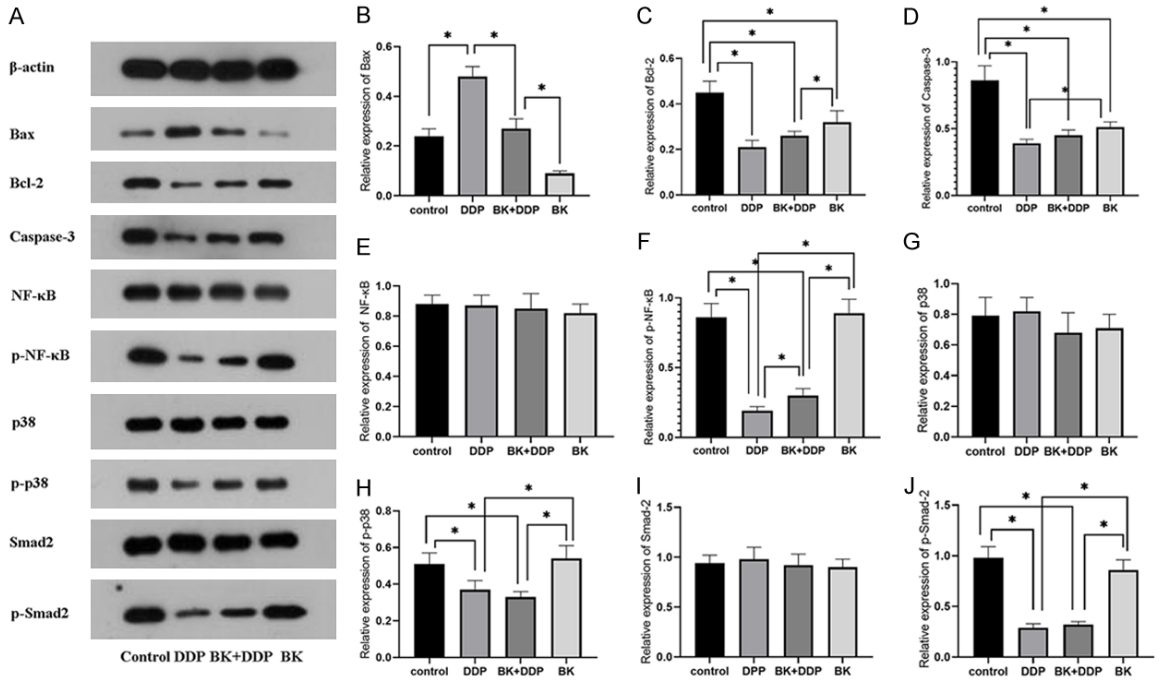

Figure 7. The protein expressions detected by Western blot. A. Results of Western blot; B-J. Statistical chart of Western blot. Compared with those in the control group, the expressions of Bcl-2, Caspase-3, p-NF-κB, p-p38 and p-Smad2 of GP-H1 cells were lower in the DDP group, while Bax was higher ($P < 0.05$). Compared with those in the DDP group, the expressions of Bcl-2, Caspase-3, p-NF-κB, p-p38 and p-Smad2 of GP-H1 cells were higher in the BK+DDP group and the BK group, while Bax was lower ($P < 0.05$). DDP: cisplatin; BK: bradykinin. * indicates pairwise comparison, $P < 0.05$.

There were no statistically significant differences in the expressions of NF-κB, p38 and Samd2 among different groups (**Figure 7**).

Effect of PI3K/Akt/NO signaling pathway on BK protection against DDP-induced myocardial injury

Four inhibitors were used in addition to BK and DDP: PLC inhibitor U-73122 (U), B2 receptor inhibitor HOE-140 (H), NOS inhibitor L-NAME (L) and PI3K inhibitor LY294002 (LY). It was revealed that cell survival was decreased in all cases compared with the BK+DDP group, and the protective effect of BK against DDP-induced myocardial injury was attenuated (**Figure 8**).

Effect of the PI3K/Akt/NO signaling pathway on the reduction of DDP-induced elevation of ROS by BK

According to the above grouping and administration method, laser confocal microscopy was used to detect intracellular ROS levels, and all four inhibitors exhibited inhibitory effect of BK on reducing ROS levels induced by DDP in cardiomyocytes (**Figure 9**).

Effect of the PI3K/Akt/NO signaling pathway on BK mitigation of DDP-induced MMP reduction

GP-H1 cells were grouped and administered according to the above methods, and laser confocal microscopy was used to detect cellular MMP. It was found that the BK mitigation of DDP-induced decrease in cellular MMP was blocked by the use of the four antagonists (**Figure 10**).

Discussion

DDP has been widely applied in cancer treatment, because it can inhibit DNA and RNA synthesis and has a strong anti-tumor activity in a wide range of antimicrobial spectrum [11]. Previous studies have shown that DDP can increase the serum levels of CK, CK-MB, AST, ALT and LDH. At a pathological level, it has been indicated that myocardial tissue shows

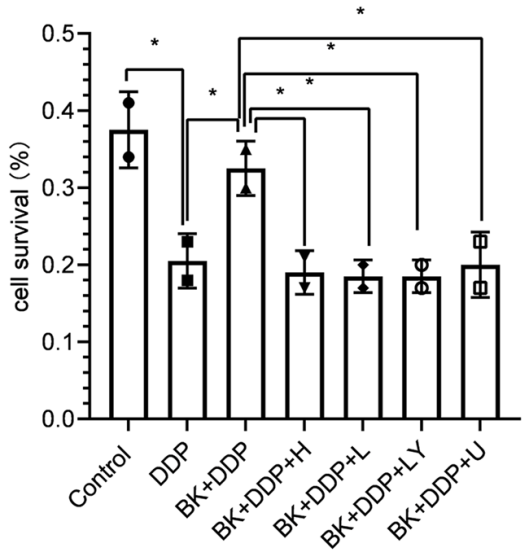

Figure 8. Effect of PI3K/Akt/NO signaling pathway on BK's protection against DDP-induced myocardial injury. Compared with that in the control group, the survival rate of GP-H1 cells was lower in the other six groups ($P < 0.05$). Compared with that in the BK+DDP group, the survival rate of GP-H1 cells was lower in other four groups ($P < 0.05$). DDP: cisplatin; BK: bradykinin. *$P < 0.05$.

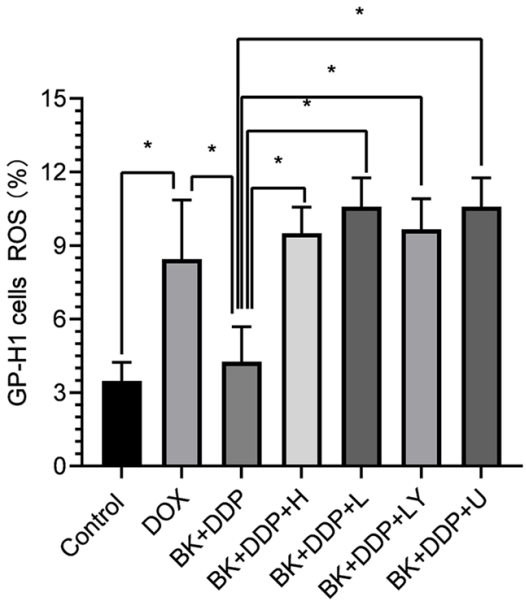

Figure 9. Effect of the PI3K/Akt/NO signaling pathway on the increase in ROS caused by BK lowering DDP. Compared with that in the control group, the ROS activity of GP-H1 cells was higher in the DDP group and the four inhibitor groups ($P < 0.05$). The ROS activity of GP-H1 cells was lower in the BK+DDP group ($P < 0.05$) compared with those in the other five groups administered with the drug. DDP: cisplatin; BK: bradykinin; ROS: reactive oxygen species. *$P < 0.05$.

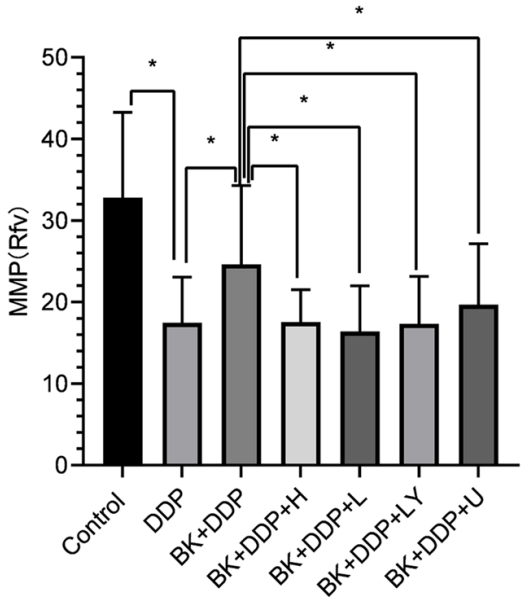

Figure 10. Effect of PI3K/Akt/NO signaling pathway on BK's mitigation of DDP-induced MMP reduction. Compared with the control group, the other six groups had decreased MMP levels ($P < 0.05$), and compared with the BK+DDP group, the other five groups had lower MMP levels ($P < 0.05$). DDP: cisplatin; BK: bradykinin; MMP: Mitochondria Membrane Potential. *$P < 0.05$.

capillary edema and stasis after DDP administration, changes in vacuolar degeneration, and inflammatory cell infiltration, which are considered as precursors of heart failure [12, 13].

In this study, the cellular analysis in vitro showed that DDP reduced the survival rate of GP-H1 cells. Also, higher DDP concentration and longer duration of action led to more pronounced reduction in survival rate. Most eukaryotic cells generate ROS in mitochondria, and during aerobic respiration, the activated NADPH oxidase complex binds to NADPH and releases two electrons, which are delivered via flavin adenine dinucleotide to ferrous heme, and further binds two oxygen molecules outside the cytosol to generate O_2^-, finally generating other types of superoxide molecules via multiple electron transfer [14, 15]. Oxidative stress leads to a rapid increase of ROS, which causes the peroxidation of a variety of biomolecules and damages biofilms, and these oxidation products are converted into MDA by oxidase [16, 17]. In this study, the effects of DDP and BK on ROS in GP-H1 cells were detected by fluorescence staining method, and it was found that DDP increased the ROS level in GP-H1

cells, but when these cells were pretreated with BK before DDP treatment, the ROS level did not continue to increase. BK could inhibit the increase of MDA level induced by DDP. The SOD activity of antioxidant enzymes was decreased significantly in the DDP group, and was increased again with the induction of BK. Therefore, it is suggested that the enhanced oxidative stress induced by DDP is a critical cause of myocardial disease, and BK can regulate the intracellular oxidative stress to control the cardiotoxicity of DDP.

Mitochondria are vulnerable to ROS attack caused by oxidative stress response. ROS attacks mitochondria, causing biomolecular peroxidation on the bilayer biofilm, altering membrane permeability, leading to calcium outflow and promoting the release of cytochrome C [18, 19]. Studies have suggested that the apoptosis induced by mitochondrial injury is an important cause of DDP-induced cardiotoxicity [20]. The signals regulating apoptosis source both from external and internal pathways, with the latter being the mitochondrial apoptosis pathway, in which Bcl-2 family proteins are vital regulators [21]. The Bcl-2 family proteins can be recognized intra- and intermolecularly to form trimeric structures with good stability and regulate the formation of ion channels, ultimately exerting anti-apoptosis effects [22, 23]. In the Bcl-2 protein family, Bax is a pro-apoptotic protein, which can resist the protective effect of Bcl-2 and accelerate apoptosis if overexpressed [24]. A previous study has shown that DDP can reduce the MMP level of GP-H1 cells, and BK can control the MMP decline [25]. The present study analyzed the influence of DDP and BK on MMP in GP-H1 cells. We found that DDP significantly reduced the MMP levels of GP-H1 cells. When BK was used for pretreatment, the MMP level did not continue to decline, indicating that BK could inhibit the damage of cell mitochondria induced by DDP and play a role in protecting cell mitochondria. Further monitoring of GP-H1 cell apoptosis revealed that Bax/Bcl-2 elevation, Caspase-3, p-NF-κB, p-p38 and p-Smad2 suppression and apoptosis were significant after DDP treatment, but the changes were reversed by pretreatment with BK, indicating that BK could inhibit the apoptosis induced by DDP. A relevant study has also shown that DDP can increase Bax/Bcl-2 and promote apoptosis [26]. Studies on BK showed that its cardioprotective effect was mainly due to the ability of B2 receptor to mediate endothelial NOS activation and produce NO [27]. Evidence has shown that Akt activation can promote the production of NO in endothelial cells, inhibit the formation of DDP-induced cardiomyocyte apoptosis, and also prevent cardiac dysfunction [28]. During the apoptosis, Bcl-2 is located on the mitochondrial membrane and is an anti-apoptotic protein downstream of the PI3k/Akt pathway. The activation of the PI3k/Akt/NO pathway can also inhibit the formation of apoptosis [29]. In the present study, the treatment with four inhibitors revealed that BK could inhibit the DDP-induced enhancement of cellular oxidative stress, the increased apoptosis and the reduced cell survival rate.

However, there are some shortcomings in this study, which are reflected in the lack of in-depth study on the mechanism of action, and this shortcoming will be improved in future studies.

In summary, BK can play a protective role against cardiomyocyte injury induced by DDP, which is mainly because BK can activate PI3k/Akt/NO signaling pathway, leading to a reduction of DDP-induced oxidative stress and a decrease in apoptosis elevation.

Disclosure of conflict of interest

None.

Address correspondence to: Suwen Su, School of Basic Medical Sciences, Hebei Medical University, No. 361, Zhongshan East Road, Shijiazhuang 050032, Hebei, China. Tel: +86-15232111665; E-mail: 2856325691@qq.com; Zengjuan Liu, Department of Pharmacy, The Third Hospital of Shijiazhuang, No. 15, Tiyu South Street, Shijiazhuang 050011, Hebei, China. Tel: +86-13323110819; E-mail: liuzengjuan819@126.com

References

[1] Gunturk EE, Yucel B, Gunturk I, Yazici C, Yay A and Kose K. The effects of N-acetylcysteine on cisplatin induced cardiotoxicity. Bratisl Lek Listy 2019; 120: 423-428.

[2] Cao BB, Li D, Xing X, Zhao Y, Wu K, Jiang F, Yin W and Li JD. Effect of cisplatin on the clock genes expression in the liver, heart and kidney.

Biochem Biophys Res Commun 2018; 501: 593-597.
[3] Adalı F, Gonul Y, Kocak A, Yuksel Y, Ozkececi G, Ozdemir C, Tunay K, Bozkurt MF and Sen OG. Effects of thymoquinone against cisplatin-induced cardiac injury in rats. Acta Cir Bras 2016; 31: 271-277.
[4] Xu J, Zhang B, Chu Z, Jiang F and Han J. Wogonin alleviates cisplatin-induced cardiotoxicity in mice via inhibiting gasdermin D-mediated pyroptosis. J Cardiovasc Pharmacol 2021; 78: 597-603.
[5] Hanchate LP, Sharma SR and Madyalkar S. Cisplatin induced acute myocardial infarction and dyslipidemia. J Clin Diagn Res 2017; 11: OD05-OD07.
[6] Lancellotti P, Ancion A, D'Orio V, Gach O, Maréchal P and Krzesinski JM. Bradykinin and cardiovascular protection. Role of perindopril, an inhibitor of angiotensin conversion enzyme. Rev Med Liege 2018; 73: 197-205.
[7] Nokkari A, Abou-El-Hassan H, Mechref Y, Mondello S, Kindy MS, Jaffa AA and Kobeissy F. Implication of the kallikrein-kinin system in neurological disorders: quest for potential biomarkers and mechanisms. Prog Neurobiol 2018; 165-167: 26-50.
[8] Bhoola KD, Figueroa CD and Worthy K. Bioregulation of kinins: kallikreins, kininogens,and kininases. Pharmacol Rev 1992; 44: 1-80.
[9] Kenne E, Rasmuson J, Renné T, Vieira ML, Müller-Esterl W, Herwald H and Lindbom L. Neutrophils engage the kallikrein-kinin system to open up the endothelial barrier in acute inflammation. FASEB J 2019; 33: 2599-2609.
[10] Sharma JN. The kinin system in hypertensive pathophysiology. Inflammopharmacology 2013; 21: 1-9.
[11] Meredith AM and Dass CR. Increasing role of the cancer chemotherapeutic doxorubicin in cellular metabolism. J Pharm Pharmacol 2016; 68: 729-741.
[12] Kalam K and Marwick TH. Role of cardioprotective therapy for prevention of cardiotoxicity with chemotherapy: a systematic review and meta-analysis. Eur J Cancer 2013; 49: 2900-2909.
[13] Patanè S. Cardiotoxicity: cisplatin and long-term cancer survivors. Int J Cardiol 2014; 175: 201-202.
[14] Brieger K, Schiavone S, Miller FJ Jr and Krause KH. Reactive oxygen species: from health to disease. Swiss Med Wkly 2012; 142: w13659.
[15] Liochev SI. Reactive oxygen species and the free radical theory of aging. Free Radic Biol Med 2013; 60: 1-4.
[16] Finkel T. Signal transduction by reactive oxygen species. J Cell Biol 2011; 194: 7-15.
[17] Dryden M. Reactive oxygen species: a novel antimicrobial. Int J Antimicrob Agents 2018; 51: 299-303.
[18] Van Acker H and Coenye T. The role of reactive oxygen species in antibiotic-mediated killing of bacteria. Trends Microbiol 2017; 25: 456-466.
[19] Hrycay EG and Bandiera SM. Involvement of cytochrome P450 in reactive oxygen species formation and cancer. Adv Pharmacol 2015; 74: 35-84.
[20] Cao D, Zhang X, Akabar MD, Luo Y, Wu H, Ke X and Ci T. Liposomal doxorubicin loaded PLGA-PEG-PLGA based thermogel for sustained local drug delivery for the treatment of breast cancer. Artif Cells Nanomed Biotechnol 2019; 47: 181-191.
[21] Estaquier J, Vallette F, Vayssiere JL and Mignotte B. The mitochondrial pathways of apoptosis. Adv Exp Med Biol 2012; 942: 157-183.
[22] Wang X, Lu X, Zhu R, Zhang K, Li S, Chen Z and Li L. Betulinic acid induces apoptosis in differentiated PC12 cells via ROS-mediated mitochondrial pathway. Neurochem Res 2017; 42: 1130-1140.
[23] Lopez J and Tait SW. Mitochondrial apoptosis: killing cancer using the enemy within. Br J Cancer 2015; 112: 957-962.
[24] Kvansakul M, Caria S and Hinds MG. The Bcl-2 family in host-virus interactions. Viruses 2017; 9: 290.
[25] Delbridge AR, Grabow S, Strasser A and Vaux DL. Thirty years of BCL-2: translating cell death discoveries into novel cancer therapies. Nat Rev Cancer 2016; 16: 99-109.
[26] Raaymakers C, Verbrugghe E, Stijlemans B, Martel A, Pasmans F and Roelants K. The anuran skin peptide bradykinin mediates its own absorption across epithelial barriers of the digestive tract. Peptides 2018; 103: 84-89.
[27] Maurer M, Bader M, Bas M, Bossi F, Cicardi M, Cugno M, Howarth P, Kaplan A, Kojda G, Leeb-Lundberg F, Lötvall J and Magerl M. New topics in bradykinin research. Allergy 2011; 66: 1397-1406.
[28] Yousefpour P, Ahn L, Tewksbury J, Saha S, Costa SA, Bellucci JJ, Li X and Chilkoti A. Conjugate of doxorubicin to albumin-binding peptide outperforms aldoxorubicin. Small 2019; 15: e1804452.
[29] Torrealba N, Rodriguez-Berriguete G, Fraile B, Olmedilla G, Martínez-Onsurbe P, Sánchez-Chapado M, Paniagua R and Royuela M. PI3K pathway and Bcl-2 family. Clinicopathological features in prostate cancer. Aging Male 2018; 21: 211-222.